Send Orders for Reprints to reprints@benthamscience.ae

158 *Current Cancer Drug Targets*, 2015, 15, 158-170

Identification of VEGFR2-Binding Peptides Using High Throughput Bacterial Display Methods and Functional Assessment

Kefeng Pu[a,b,c,#], Lihua Yuan[a,#], Lisha Chen[a,b,c], Anxin Wang[a,b,c], Xuan Zhou[a], Hailu Zhang[d] and Yimin Zhu[a,*]

[a]*Key Laboratory for Nano-Bio Interface Research, Suzhou Key Laboratory for Nanotheranostics, Division of Nanobiomedicine, Suzhou Institute of Nano-Tech and Nano-Bionics, Chinese Academy of Sciences, Suzhou 215123, China;* [b]*Institute of Biophysics, Chinese Academy of Science, Beijing 100101, China;* [c]*University of the Chinese Academy of Sciences, Beijing 100049, China;* [d]*Laboratory of Magnetic Resonance Spectroscopy and Imaging, Suzhou Institute of Nano-Tech and Nano-Bionics, Chinese Academy of Sciences, Suzhou 215123, China*


Kefeng Pu

Abstract: The signal transduction pathway initiated by vascular endothelial growth factor-vascular endothelial growth factor receptor 2 (VEGF-VEGFR2) plays an important role in the angiogenesis of tumors. The effective antagonists of VEGFR2 would behave as potent drugs for the treatment of malignant cancers. In our study, specific binding peptides with high affinity to VEGFR2 were obtained through bacterial display technology. Conserved motif (FF/YEXWGVK) among those peptide sequences was discovered. One of the selected peptides, VRBP1 (YDGNSFYEMWGVKPASES) was identified by screening the biased bacterial peptide library and its physiochemical feature was further characterized. The results of surface plasmon resonance (SPR) assay indicated that the dissociation constant (K_D) value of VRBP1 was 228.3 nM and this peptide competed with VEGF binding to VEGFR2. Particles conjugated with VRBP1 could recognize the human umbilical vein endothelial cells (HUVEC) which express VEGFR2 on the surface. Further therapeutic effect of VRBP1 was examined by *in vivo* experiments. VRBP1 could result in a significant decrease in tumor size of H460 xenografts. The results from the immunohistochemical assay showed that CD31 positive signals in VRBP1-treated group were fewer than those in the control ones. These data highlighted the potential of VEGFR2-binding peptides as effective molecules for cancer diagnosis and therapy.

Keywords: Angiogenesis, bacterial surface display, cancer diagnosis, cancer therapy, peptide, vascular endothelial growth factor receptor 2 (VEGFR2).

INTRODUCTION

Angiogenesis is a normal process occurring during embryonic and post-embryonic development, reproductive cycle and wound repair. Now, many data have shown that angiogenesis plays a critical role in cancer development, especially in the rapid growth of solid tumors beyond 1-2 mm in diameter and metastatic tumors [1, 2]. Studies on cancer patients have shown a direct correlation between the density of tumor vessels and an adverse prognosis [3, 4], so the development of specific anti-angiogenic agents arises as an attractive approach for the treatment of cancer and other angiogenesis-dependent diseases [4]. Vascular endothelial growth factor (VEGF) as an endothelial cell-specific mitogen has been found to be the most important angiogenic factors in tumor angiogenesis [5-7]. VEGF functions by binding to one of its specific tyrosine kinase receptors: VEGFR1 (fms-like tyrosine kinase/Flt1) [8-10], VEGFR2 (a kinase insert domain-containing receptor/KDR) [10, 11] and VEGFR3 (Flt-4) [12, 13] to promote either physiologic or pathologic angiogenesis. Only homodimerization of VEGFR2 leads to a strong autophosphorylation and it exhibits a strong induction in angiogenesis [14, 15], while VEGFR1 participates in transduction of a weak angiogenic signal [14]. Furthermore, VEGFR2 is usually found to be aberrantly expressed or constitutively phosphorylated in tumors [16-18]. Recently, Sorafenib [18, 19], an anti-VEGFR2 antagonist was introduced to the market for cancer treatment. Although antibodies targeting the different cancer-related molecules have already been used in cancer therapy successfully [20], some targeting molecules such as peptides have presented numerous advantages over antibodies and may be used as substitutes for antibodies in future. For example, peptides have smaller sizes and better tissue penetration than antibodies, and coupling drugs or imaging agents with peptides is easier than that with antibodies [21, 22]. In addition, peptides represent alternatives to antibodies in terms of maximizing safety and minimizing production costs [21, 23].

Phage display technology or chemical synthesis has been successfully used to obtain the requisite peptides [24-26]. Several VEGFR2-binding peptides have been identified using phage display method [27, 28], but no consensus sequences were discovered and their affinity and specificity to VEGFR2 still need to be improved for the clinical use. Therefore, it is necessary to develop more specific binding peptides to VEGFR2 with high affinity for cancer diagnosis and therapy. In our study, we applied bacterial display

*Address correspondence to this author at 398 Ruoshui Road, Suzhou Industrial Park, Suzhou 215123, China; Tel: +86 512 6287 2618; Fax: +86 512 6287 2792; E-mail: ymzhu2008@sinano.ac.cn

[#]These authors contributed equally to this work.

1873-5576/15 $58.00+.00

method to identify the specific binding peptides for extracellular domain of VEGFR2. Bacterial display method coupled with fluorescence-activated cell sorting (FACS) technology is a simpler, more effective, high throughput and more quantitative approach to discover and optimize peptides comparing with phage display methods [29-31]. In this study, a specifically VEGFR2 binding peptide with moderate affinity was identified. It not only inhibited proliferation of human umbilical vein endothelial cells (HUVEC) *in vitro*, which express VEGFR2 on their surface [32], but also reduced the tumor growth of H460 xenografts *in vivo*. Therefore, this peptide has the potential to be used as an effective molecule for cancer diagnosis and therapy.

MATERIALS AND METHODS

Bacterial Strains, Cell Lines and their Growth Conditions, Plasmids and Reagents

A library of peptides with 15 randomized amino acids (X_{15}) on eCPX scaffold including 2×10^9 members used in this study was a gift from Patrick S. Daugherty in the Department of Chemical Engineering, University of California, Santa Barbara [33]. Recombinant human $VEGF_{165}$ ($rhVEGF_{165}$) was purchased from Beijing ZhongKeWuYuan Biotechnology (http://www.zkwysw.com). Recombinant human VEGFR1, VEGFR2 and VEGFR3 were purchased from Sino Biological Inc (http://www.sinobiological.com). Streptavidin R-phycoerythrin (SAPE) (Cat No. 1148354), Dynabeads MyoneTM Carboxylic Acid (Cat No. 65011) and MyOne streptavidin-coated magnetic microbeads (Cat No. 650.01) were bought from Invitrogen. IgG and human serum was purchased from Sigma. Fetal bovine serum (FBS), Dulbecco's modified Eagle's high glucose medium (DMEM/high), RPMI-1640 medium and Medium 199 (M199) were purchased from Thermo (Hyclone Corp., USA). Peptides in this article were synthesized by Shanghai Bioengineering Ltd. Bovine serum albumin (BSA), chloramphenicol (CM), penicillin/streptomycin and D-(+)-glucose were purchased from China National Medicine Corp. Superparamagnetic iron oxide particle (SPIO) was a gift from Dr. Yu Zhang (Southeast University, China) [34].

HLF (human lung fibroblast) cells were grown in DMEM/ high medium and human lung cancer cells (H460) were cultured in RPMI-1640 medium in a 5% CO_2 humidified incubator at 37 °C. The medium was supplemented with 10% FBS and 1% penicillin/streptomycin. H460 and HLF cells were kind gifts from Dr. Biliang Zhang (Guangzhou institutes of biomedicine and health, CAS, China).

The HUVEC cells were separated and cultured according to the procedure described by Maruyama *et al*. [35, 36]. HUVEC cells were maintained in M199 in a 5% CO_2 humidified incubator at 37 °C. The medium was supplemented with 20% FBS and 1% penicillin/streptomycin. Tumor cell lines were authenticated by short tandem repeat (STR) analysis.

Screening of Binding Peptides to VEGFR2 from a Random Library

Biotinylation of VEGFR2 was performed using the FluoReporter mini-biotin-XX protein labeling kit (Invitrogen Corp., CA, USA, Cat No. F-6347) and following its instruction. A library of peptides with 15 randomized amino acids was used for screening the binding peptides to VEGFR2. Frozen aliquots of 2×10^{10} bacteria were thawed and cultivated overnight with shaking at 200 rpm in super optimal broth (SOB) at 37 °C with 34 mg/mL CM and 0.2% (w/v) D-(+)-glucose added. The next day, bacteria were sub cultured at 1:50 in lysogeny broth (LB) medium supplemented with 34 mg/mL CM for 2 h at 37 °C followed by induction with 0.02% (w/v) L-(+)-arabinose for 1 h at room temperature to ensure peptides expressed on the surface of bacteria [33]. Magnetic-activated cell sorting (MACS) was first performed with 100 nM biotinylated VEGFR2 to reduce the library size and ratio of beads: bacteria was 1:2, as previously described [29, 37]. Afterwards, the library was incubated with biotinylated VEGFR2 at various concentrations from 20 nM to 50 nM for 45 min at 4 °C with or without co-incubated with 20 μM human IgG. After washing with 1 mL phosphate-buffered saline (PBS, pH 7.4) for three times and 100 μL (3.3 nM) SAPE was added into the tube, bacteria clones with high fluorescence intensity, meaning that peptides expressed on the bacteria surface could bind with VEGFR2, were sorted. These sorted bacteria clones were used for the next round of screening.

A few rounds of FACS were performed and when the fluorescent signals of bacteria stopped increasing in the two sequential rounds, *i.e.*, when the binding bacteria clones for VEGFR2 were fully enriched, the screening procedure for the binding peptides was terminated. Sorted bacteria with binding peptides were cultured on LB medium plate containing 1% agar and 34 mg/mL CM. After culturing for 16 h at 37 °C, monoclonal bacteria were picked and cultured in 5 mL SOB containing 34 μg/mL CM at 37 °C overnight. The sequences of the peptides showed on these clones were obtained by sending these bacteria to Sangon Biotech Co., Ltd. Shanghai, China. for sequencing.

Determination of Binding Activity for Peptides-Bacteria with VEGFR2

The preliminary examination of peptides-bacteria binding properties was performed under different treatment conditions: tough washing and serum or IgG blocking during incubation process. Individual clones including 1×10^7 bacteria induced by 0.02% (w/v) L-(+)-arabinose for 1 h at room temperature were incubated with 67 nM biotinylated VEGFR2 with or without 10% serum or 20 μM human IgG for 45 min at 4 °C. The bacteria were centrifuged at 3000×*g* for 5 min and washed with PBS. Sediments were resuspended in 100 μL SAPE and incubated for 20 min at 4 °C. Prior to analysis, bacteria were centrifuged at 3000×*g* for 5 min and resuspended in 1 mL PBS, with or without three extra washes. The binding of VEGFR2 was assessed *via* reading of fluorescent intensities of bacteria by flow cytometry.

K_D Measurement of Peptides-Bacteria to VEGFR2

Biotinylated VEGFR2 at various concentrations of 0.5 nM, 1 nM, 5 nM, 15 nM, 40 nM and 60 nM was incubated with induced bacteria clones and the fluorescent intensities were recorded by flow cytometry. The relative binding affinity (K_D value) was estimated by formula $Fl\text{-}Fl_{eCPX}=Fl_{max}$

[P]/(K_D+[P]). Fl is the fluorescent value produced by individual bacteria clones incubated with VEGFR2. Fl_{eCPX} indicates the fluorescent intensities of eCPX bacteria after incubation with VEGFR2. Fl_{max} represents the highest fluorescent value of bacteria-VEGFR2 complex and [P] is the concentration of VEGFR2.

Enzyme-Linked Immunosorbent Assay (ELISA) with Fluorescein Isothiocyanate (FITC)-Conjugated Peptides

VEGFR2 (2μg/mL in PBS buffer, pH 7.4) was coated on 96-well plates (50 μL/well) and kept at 4 °C overnight. These wells were washed with PBS and then blocked with 3% BSA in PBS with 0.05% Tween20, for1 h at room temperature. FITC-conjugated VRBP1 and control peptide (CONP, GSSGSSGSSGSSGSSGSSGSSGSSK) at a concentration of 20 μM in PBS were added and incubated at room temperature for 30 min. After washing with PBS, fluorescence intensity was measured by VICTOR X4 Multilabel Reader (PerkinElmer Life and Analytical Sciences, Boston, MA, USA).

Examination of Peptides Binding Activity to HUVEC Cells *in vitro*

These experiments were performed on both attached and detached HUVEC cells. The fluorescence microscopy experiment was carried out to examine the binding efficiency of synthesized FITC-conjugated peptides with attached HUVEC cells. HUVEC cells were seeded in 12-well plates (Costa, corning incorporated) at a density of 1×10^5 cell/well overnight and fixed with 4% paraformaldehyde at room temperature for 10 min. After washing, cells were blocked with a culture medium containing 5% BSA at 37 °C for 10 min and then incubated with FITC-conjugated peptides in serum-free medium at 37 °C for 1 h. The plates were visualized under a fluorescent microscope (Nikon Diaphot, Nikon Corp., Tokyo, Japan). The binding activity between synthesized FITC-conjugated peptides with detached HUVEC cells was determined by flow cytometry. Cultured (48 h post-seeding) HUVEC cells were harvested and resuspended in tubes. 1×10^7 HUVEC cells were incubated with 0.5 nmol FITC-conjugated peptides for 45 min on an inversion shaker at 4 °C. Cell suspensions were centrifuged at 300×*g* for 5 min at 4 °C and then washed three times with PBS. The sediment was resuspended with 1 mL PBS and immediately analyzed by FACS.

Measurement of K_D Values for Synthesized Peptides to VEGFR2

Dissociation constants of synthesized peptide were determined by SPR on a Biacore 3000 system (BIAcore AB, Uppsala, Sweden). The HRBio sensor chip (SJ Biomaterials, Suzhou, China) was activated by a 1:1 solution of 0.4 M 1-ethyl-3-(3-dimethylaminopropyl)-carbodiimide in water (EDC) and 0.1 M N-hydroxysuccinimide in water (NHS) according to the manufacturer's instructions. VEGFR2 (2-10 μg/mL in 10 mM sodium acetate, pH 5.5) was injected over the activated surfaces of flow cell 2 at a flow rate of 10 μL/min until the target immobilization levels (2,000 response units for flow cell 2) were reached. Uncoupled receptors were removed and un-reacted moieties on the chip were blocked with 1 M ethanolamine-HCl (pH 8.5). Flow cell 1 was activated and blocked without exposure to VEGFR2 and served as background control surfaces for the binding interactions.

All kinetic binding experiments were performed at 25 °C in degassed PBS running buffer (pH 7.4). Various concentrations (0.2, 0.4, 0.5 and 1 μg/mL) of peptides were flowed through the surface-immobilized VEGFR2 at 10 μL/min for 5 min and the binding events were monitored. Following association, the dissociation process of peptide-receptor complexes was monitored for 7 min.

Examination of Competence between VEGF and Peptides Binding to VEGFR2 by SPR Assay

The HRBio sensor chip was activated by a 1:1 solution of EDC/NHS. The activated surfaces of flow cell 2 were passed over by 10 μg/mL VEGFR2 at a rate of 10 μL/min until the 2000 response units (RU) were reached. After the immobilization of VEGFR2, binding peptides at a concentration of 10 μg/mL were injected at a rate of 10 μL/min followed by 3 μg/mL VEGF passed over at a rate of 10 μL/min. In another chip, the 3 μg/mL VEGF was injected followed by 10 μg/mL binding peptides passed over. The RU was monitored in real-time and presented in a sensorgram of RU versus time.

Competitive Binding Assay of VEGF to VEGFR2 with ELISA

VEGFR2 was coated onto 96-well plates as described above. FITC-conjugated VRBP1 at a concentration of 20 μM in PBS was mixed with VEGF at different concentrations (0, 0.05, 0.1, 0.2, 0.4, 0.8, 1 and 2 ng/mL) and added to wells. After 30 min of incubation at room temperature, the wells were washed and FITC-conjugated VRBP1 bound to VEGFR2 was measured by VICTOR X4 Multilabel Reader.

MTT Assay

The blocking activity of peptides to VEGFR2 was evaluated by methyl thiazolyltetrazolium (MTT) assay. HUVEC cells were plated into 96-well tissue culture plates (Costa, corning Corp., USA) at a density of 8000 cells per well and cultured overnight. After that, cells were serum starved for another 24 h. In the serum free medium, $rhVEGF_{165}$ (30 ng/mL) alone or $rhVEGF_{165}$ together with peptides ranging from 5 μg/mL to 50 μg/mL was introduced into wells for 48 h. Twenty μL MTT (5 mg/mL) was added to each well and incubated for another 4 h. The supernatant was removed followed by adding 150 μL dimethyl sulfoxide (DMSO) in order to dissolve the formed water-insoluble formazan crystals. Reading of optical density (OD) at 490 nm was obtained from VICTOR X4 Multilabel Reader.

Conjugation Experiments of Peptides with Dynabeads or Superparamagnetic Iron Oxide Particles (SPIO)

Dynabeads MyoneTM Carboxylic Acid with an average diameter of 1.06 μm and SPIO with an average diameter of 20 nm were used to perform the peptides conjugation experiment. A mixture of EDC (20 mg/mL) and NHS (1.2 mg/mL) in 0.1 M 2-(N-morpholino)-ethanesulfonic acid

(MES) was used to activate the surface of Dynabeads and SPIO for 15 min. Then the peptides were added and incubated 8 h at 4 °C. The peptides used in the conjugation experiment contained "GSSGSSK" linkers at the C-terminal.

Evaluation of the Targeting Effect of Peptides to VEGFR2 by Trapping Experiments

HUVEC cells, HLF cells (as a control cell which expressed VEGFR2 at a low level) were plated into 24-well cell culture plate at a concentration of 3×10^4 cells per well (Costa, corning Corp., USA). Ten μL Dynabeads coupled with different peptides were re-suspended in 200 μL PBS and added into wells. During the incubation process, the plate was shaken every 30 seconds for 10 min. Afterwards, each well was washed 3 times with PBS. The targeting effects of peptides to VEGFR2 were evaluated by comparing the amount of cells with different peptide treatments under the inverted microscope (Nikon Diaphot, Nikon Corp., Tokyo, Japan).

Evaluation of Targeting Effect of Peptides to VEGFR2 by MRI (Magnetic Resonance Imaging) Detection

HUVEC cells and HLF cells, at a density of 0.5×10^6 cells per well in a 6-well plate, were washed and trypsinized after incubation with SPIO at a final Fe concentration of 0, 19, 38, and 76 μg/mL for 2 h. Cells were collected by centrifugation at 300×*g* for 5 min. The obtained cells were suspended in 1% agar in 500 μL PBS and the mixtures were injected into the NMR tubes and detected as follows. T2 weighted images were acquired using multi-slice multi-echo (MSME) protocol on a 11.7 T Bruker micro 2.5 micro-MRI system with the following parameters: repetition time (TR) = 5000 ms, echo time (TE) = 80 ms, imaging matrix = 128×128, slice thickness = 1.5 mm and field of vision (FOV) = 2.20 cm × 2.20 cm.

Construction of Tumor Mice Models with Subcutaneous Xenograft

The nu/nu mice (female, 3-4 weeks old) were obtained from Nanjing Sikerui Biological Technology Co., Ltd. Mice were maintained under super pathogen-free conditions and housed in barrier facilities on a 12h light/dark cycle, with food and water ad libitum. The mice were maintained as per the principles and guidelines of the ethical committee for animal care in accordance with the China National Law on animal care and use. Cultured tumor cells (H460) were implanted subcutaneously (sc) into the flanks of mice. When tumor volume reached 2 cm^3, mice were sacrificed and the tumor mass was divided into small pieces. A small tumor tissue about 2 mm^3 was transplanted subcutaneously into the right leg of each mouse. One day later, mice were divided randomly into 2 groups, with four mice in each group.

The Treatment of Mice with Peptides

VRBP1 and CONP were dissolved in 0.9% physiological saline. One day after tumor xenograft was transplanted to mice, 100 μL VRBP1 (400 μg/mL), CONP (400 μg/mL) or 0.9% physiological saline was injected to tumor sites subcutaneously every other day. After being injected for 11 times, mice were sacrificed and tumor tissues were put into 4% paraformaldehyde for further experiments. During treatment, the tumor size was measured and recorded in two dimensions, and the volume was calculated using the formula: tumor volume (mm^3) = 1/2 × length (mm) × width $(mm)^2$.

Immunohistochemistry and Immunofluorescence-Like Assay

For immunohistochemistry assay, the fixed tumor tissue samples were embedded in paraffin and sectioned into slices as thin as 5 μm with a microtome. Tissue sectioned at 5 μm were deparaffinized in xylene, rehydrated through graded alcohol series, and subjected to immunohistochemistry assay with a monoclonal rabbit anti-mice CD31 antibody. Antigen retrieval was done in citric acid (pH 6.0) at 95 °C for 20 min. Endogenous peroxidase activity was blocked with 3% hydrogen peroxide for 10 min, and nonspecific binding sites were blocked with 5% BSA for 30 min at 37 °C. Primary antibody to CD31 was diluted at 1:100 in PBS. Next day, goat anti-rabbit immunoglobulin antibodies labeled with horseradish peroxidase were diluted at 1:500 in PBS and incubated with sections for 45 min at 37 °C. Sections were incubated with diaminobenzidinechromogen substrate solution for 10 min and counterstained with hematoxylin. After that, sections were visualized with a Nikon Eclipse 55i microscope equipped with a Nikon DS-5M camera, using Image-Pro Plus acquisition software. 100×, 200× and 400× images were acquired.

For immunofluorescence-like assay, tissue sections from mice xenograft were incubated with 30 μM FITC labeled peptides for 45 min at room temperature after blocking with 1% BSA for 30 min. After washing with PBS three times, tumor sections were observed under fluorescence microscope.

Intratumormicrovessel Density (MVD) Accessment

MVD was assessed by light microscopic analysis for neovascular hot spots. Areas with neovascularization at the highest density were selected by scanning the tumor sections at low magnification (40× and 100× total magnification). Brown-staining microvessel counts were made on a 200×field (20×objective and 10×ocular, Nikon microscope). The value of MVD was represented with average microvessels in three 200× fields.

Statistically Analysis

All these experiments were independently replicated for three or more times and the data were presented as mean ± standard deviation (S.D.). Comparisons were carried out using Student's t-test (Microsoft Excel, Microsoft Corporation, USA). P-value < 0.05 was considered to be statistically significant.

RESULTS

Bacteria Clones Binding to VEGFR2 were Identified from a Fully Random Bacterial Peptide Library

To obtain the peptide sequences that bound specifically to VEGFR2, bacteria displaying a fully random 15-mer

peptide library (X_{15}) were incubated with VEGFR2. Bacterial libraries resulting from each cycle of screening were analyzed with flow cytometry to track enrichment. The sorting processes were carried out for 8 cycles including one round MACS (M1), and seven rounds of FACS selections. Initially, in the first two rounds of FACS selections, the concentrations of VEGFR2 were 50 nM (R1) and 20 nM (R2), and percentages of bacteria in the sorting gate were 25.1% and 38.7% (Fig. **1A**), respectively. Subsequently, the sorting strategy was changed by increasing the stringency of sorting. Following the M1, the concentration of VEGFR2 in the following screening cycles (F1 to F7, Fig. **1B**) was decreased from 50 nM to 20 nM and 20 μM human IgG was added to the screening system. In the end, 100 clones were sent for sequencing and only seven independent binding peptides sequences were obtained (clone1-clone7). A consensus sequence of FF/YEXWGVK (Fig. **2A**) was presented in most of the clones. The preliminary examination of the affinity and specificity of those peptides clones which were on the surface of bacteria for VEGFR2 was performed and in this *in situ* test, clone 1 and clone 2 kept higher fluorescent signals even under serum blocking and tough washing treatment compared with other clones (Fig. **2B**), which meant that these two clones might have higher binding affinity and specificity to VEGFR2. The apparent K_D values of bacteria clone 1 and clone 2 to VEGFR2 were 287.7 ± 0.988 nM and 312 ± 0.994 nM, respectively (Fig. **S1**).

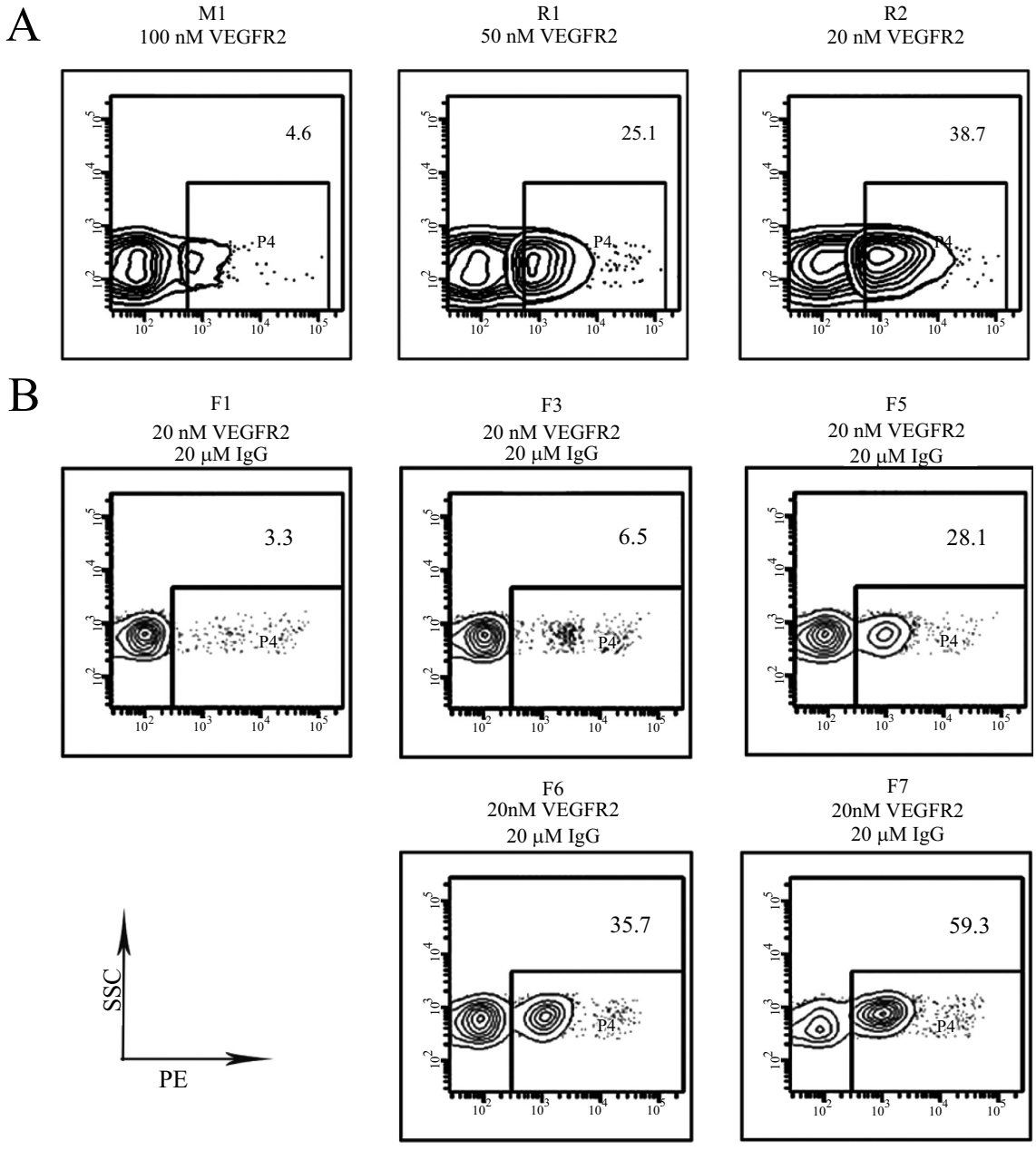

Fig. (1). The enrichment of peptide-fluorescent bacteria binding with VEGFR2. (**A**) One round of MACS with concentration of VEGFR2 at 100 nM (M1) and two rounds of FACS sorting with concentrations of VEGFR2 at 50 nM (R1) and 20 nM (R2), respectively. (**B**) Seven rounds of FACS sorting with 20 nM VEGFR2 and 20 μM human IgG (F1-F7).

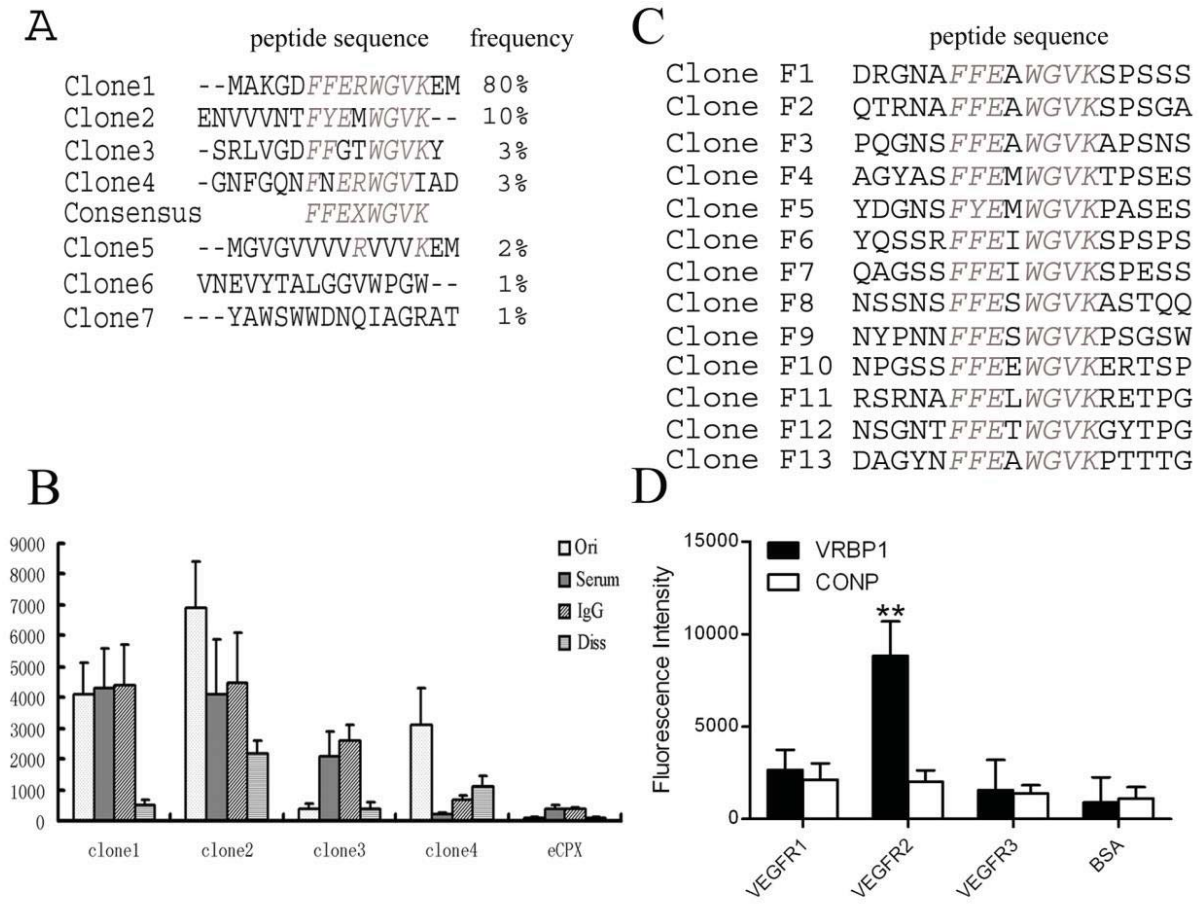

Fig. (2). The peptide sequences and binding property examination of peptides to VEGFR2. (**A**) Sequences of peptides binding to VEGFR2 from the fully random bacteria library. (**B**) The *in situ* binding property examination of peptides which were on the surface of bacteria with VEGFR2. Different treatments such as normal washing (Ori), tough washing (Diss), serum blocking (Serum) or IgG blocking (IgG) were applied. Data are presented as mean ± S.D. of three independent experiments. (**C**) Sequences of peptides binding to VEGFR2 from the focused bacteria library. (**D**) The specificity of synthesized FITC-conjugated VRBP1 using ELISA. Data are presented as mean ± S.D. of three independent experiments. **P<0.01 in comparison to 'VEGFR1', 'VEGFR3' and 'BSA' by Student's t-test.

VEGFR2 Binding Bacteria Clones with Higher Affinity and Specificity were Identified from Focused Library

In order to get higher affinity peptides and make them more suitable for application in clinic, a focused library was designed and constructed. On the N-terminus of enhanced CPX (eCPX) [33], a focused library was constructed with the form ZZZZZFF/YEXWGVKZZZZZ in which Z stood for biased amino acids except for F, L, M, V, and I. PCR was performed with CGTAGCTGGCCAGTCTGGCCAGNVSN VSNVSNVSNVSTTYTTY/TAYGARNNSTGAGGNGTN AARNVSNVSNVSNVSNVSGGAGGGCAGTCTGGGCA GTC as the forward primer, GGCTGAAAATCTTCTCTC as the reverse primer and pB33eCPX-SApep [38] as a template. The PCR product was digested with *Sfi*I and ligated into a similarly digested pB33CPX vector. The library size was 5×10^6.

Sorting experiments for VEGFR2 binding peptides were performed with 20 nM biotinylated VEGFR2 and 20 μM human IgG. After 4 rounds of sorting, a series of binding clones out of 30 random ones containing the core sequences were obtained (Fig. **2C**). The preliminary examination of the affinity and specificity of those peptides-bacteria for VEGFR2 was performed with methods similar as part of 'Determination of binding activity for peptides-bacteria with VEGFR2' in materials and methods section. Clone F5 and clone F11 (Fig. **2C**) seemed to have relatively higher fluorescent signals compared with other clones which meant that these two clones might have high binding affinity to VEGFR2 (data not shown). The peptide displayed on clone F11 (YDGNSFYEMWGVKPASES) was named as VRBP1 and that on clone F5 (RSRNAFFELWGVKRETPG) was named as VRBP2. VRBP1, VRBP2, consensus sequence FF/YEXWGVK (named as VRBCP) and CONP were synthesized with/without FITC conjugated at their N termini. The K_D value of synthesized VRBP1 to VEGFR2 was 228.3 nM measured by SPR assay. And the results of ELISA indicated that VRBP1 could specifically bind to VEGFR2 (Fig. **2D**).

VRBP1 could Recognize VEGFR2 on HUVEC Cells and Tumor Vessels

To investigate physiochemical properties of peptides sorted from bacterial library, the VEFGR2 recognizing

experiment was performed with VRBP1, VRBP2, VRBCP and CONP. Fig. **3A** showed that HUVEC cells emitted strong green fluorescent signals after incubation with FITC-conjugated VRBP1 and VRBP2, while weaker fluorescent signals on HUVEC cells incubated with VRBCP were observed. The ignorable fluorescent signals were observed on HUVEC cells when incubated with CONP.

Suspended HUVEC cells were also applied to examine the binding properties of peptides. As shown in Fig. **3B**, the percentage of the HUVEC cells binding with fluorescent labeled VRBP1 was 34.1%. HUVEC cells incubated with FITC-VRBP2 also showed reasonable high fluorescent signals, which indicated that peptides obtained from focus library could recognize HUVEC cells effectively. The percentage of the VRBCP-bound HUVEC cells was 23.2%, while that with CONP was 5%.

The binding efficiency and specificity of VRBP1 to VEGFR2 were further confirmed by the immunofluorescence-

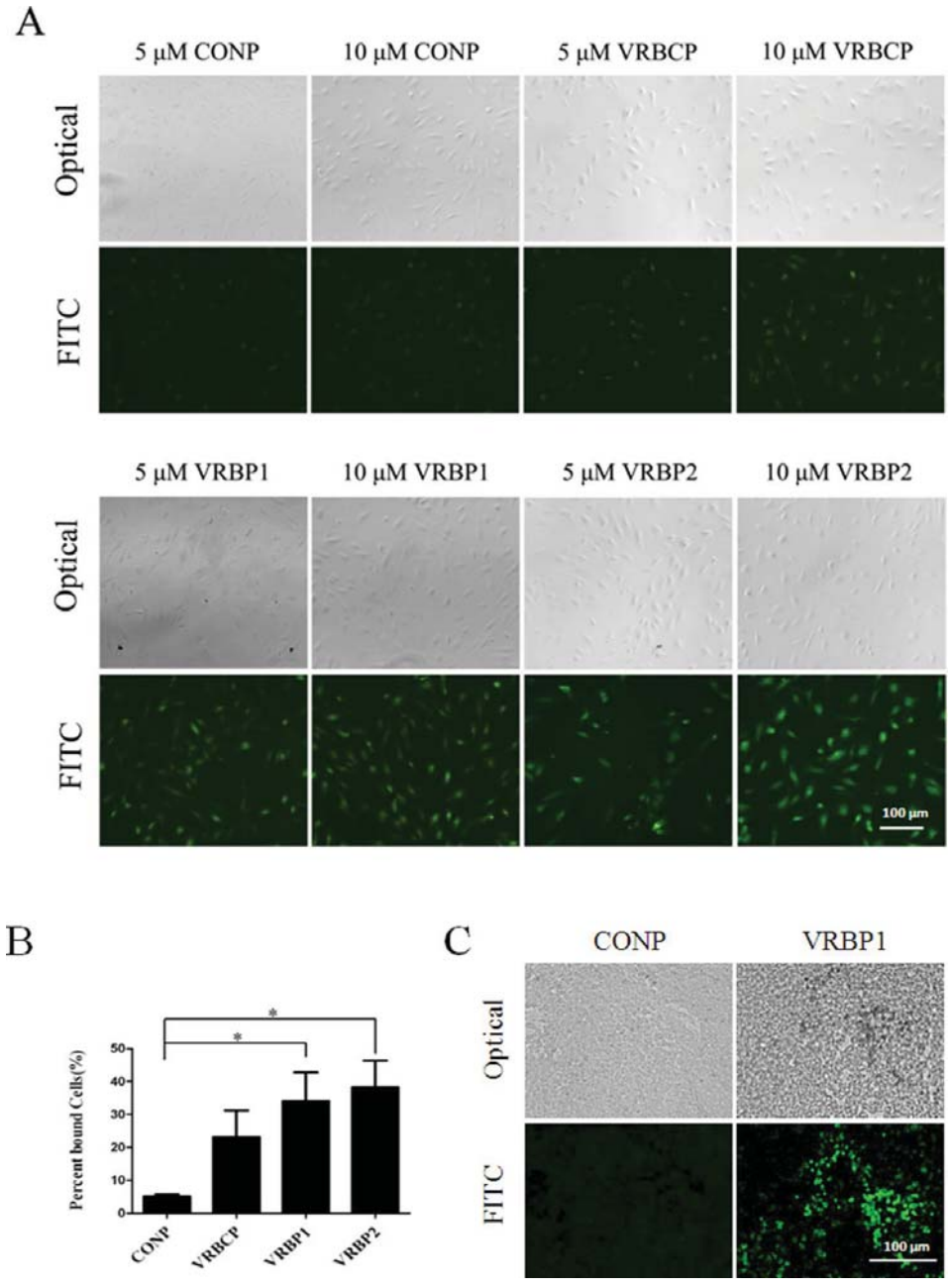

Fig. (3). Selected peptides could specifically bind to HUVEC cells *in vitro*. (**A**) HUVEC cells were incubated with FITC-conjugated CONP, VRBCP, VRBP1 and VRBP2 with concentration at 5 μM and 10 μM at 37 °C for 1 h and observed under fluorescent microscopy. (**B**) Suspended HUVEC cells were incubated with FITC-conjugated CONP, VRBCP, VRBP1 and VRBP2 at the concentration of 5 μM for 75 min at 4 °C. Cells were then subjected to flow cytometry analysis. (**C**) Tumor sections were incubated with FITC labled CONP and VRBP1. The optical and fluorescence figures were observed under fluorescence microscope. The data were presented as the mean±S.D. of three independent assays. *P<0.05 in comparison to 'CONP' by Student's t-test.

like assay with tumor sections. More green fluorescent signals were observed on the slides incubated with VRBP1, while there were ignorable signals shown up on the slides with CONP (Fig. **3C**).

VRBP1-Beads could Specifically Attach to HUVEC Cells

Since peptide VRBP1 could bind with VEGFR2 with higher affinity, the examination of the targeting function of VRBP1 was performed. The carboxylic beads coupled with VRBP1 and CONP were incubated with the HUVEC and HLF cell lines respectively at 4 °C for 10 min. After washing for 3 times with PBS, huge amount of the beads conjugated with VRBP1 on the surface was observed to be accumulated on the surface of HUVEC cells and very few on HLF cells (Fig. **4A**). Furthermore, very few of the beads conjugated with CONP were observed on both HLF and HUVEC cells (Fig. **4A**). These results indicated that the VRBP1could be used as the targeting molecules for tumor vessels in which VEGFR2 was over-expressed.

VRBP1 could Increase the Contrast Effect of MRI Examination

For verifying that the VRBP1 could work as the guiding molecule of imaging agents for cancer diagnosis, we conjugated VRBP1 and CONP with SPIO and incubated those particles with cells. The changes of magnetic signals on cells were detected with MRI machine. SPIO can produce a predominant T2 relaxation effect. SPIO-VRBP1 and SPIO-CONP at various concentrations were internalized by HUVEC cells *in vitro* and monitored by MRI. As shown in Fig. **4B**, the T2-weighted signal intensity decreased with the increase of the iron concentration. The T2-weighted images of HUVEC cells incubated with SPIO-VRBP1 appeared to be much darker than those of incubated with SPIO-CONP. Furthermore, the T2-weighted images of the HLF cells incubated with SPIO-VRBP1 showed non-changeable signals. The MRI results suggested that VRBP1 could increase the particles uptake efficiency of HUVEC cells when particles were conjugated and VRBP1 might work as effective guiding molecules for blood vessels and tumors which over-expressed VEGFR2.

VRBP1 could Competitively Bind to VEGFR2 with VEGF Examined by SPR Method and ELISA

The original SPR readout for binding of 3 μg/mL VEGF with VEGFR2 was 200.8 RU (Fig. **5A**, red line). When 10 μg/mL VRBP1 was introduced into the binding system before VEGF was added to the channel, the SPR readout of VEGF-VEGFR2 binding was decreased by 40 RU (Fig. **5A**). If 3 μg/mL VEGF was introduced into the reaction channel first before the addition of 10 μg/mL VRBP1, the SPR readout of VRBP1-VEGFR2 binding was decreased by around 34 RU (from 77.9 RU to 46.1 RU) (Fig. **5B**). The results might imply that VRBP1 bound with VEGFR2 at the same or adjacent position where VEGF bound with VEGFR2, or at other locales which could interfere the binding of VEGF to VEGFR2. The results of ELISA experiment confirmed that VRBP1 could antagonize the binding of VEGF to VEGFR2 (Fig. **S2**).

VRBP1 Specifically Inhibited the Proliferation of Vascular Endothelial Cells *in vitro*

The proliferation of endothelial cell proliferation is dependent on VEGF. Our data showed that the selected peptide VRBP1 could block VEGF binding to VEGFR2, therefore, it was necessary to examine the effect of VRBP1

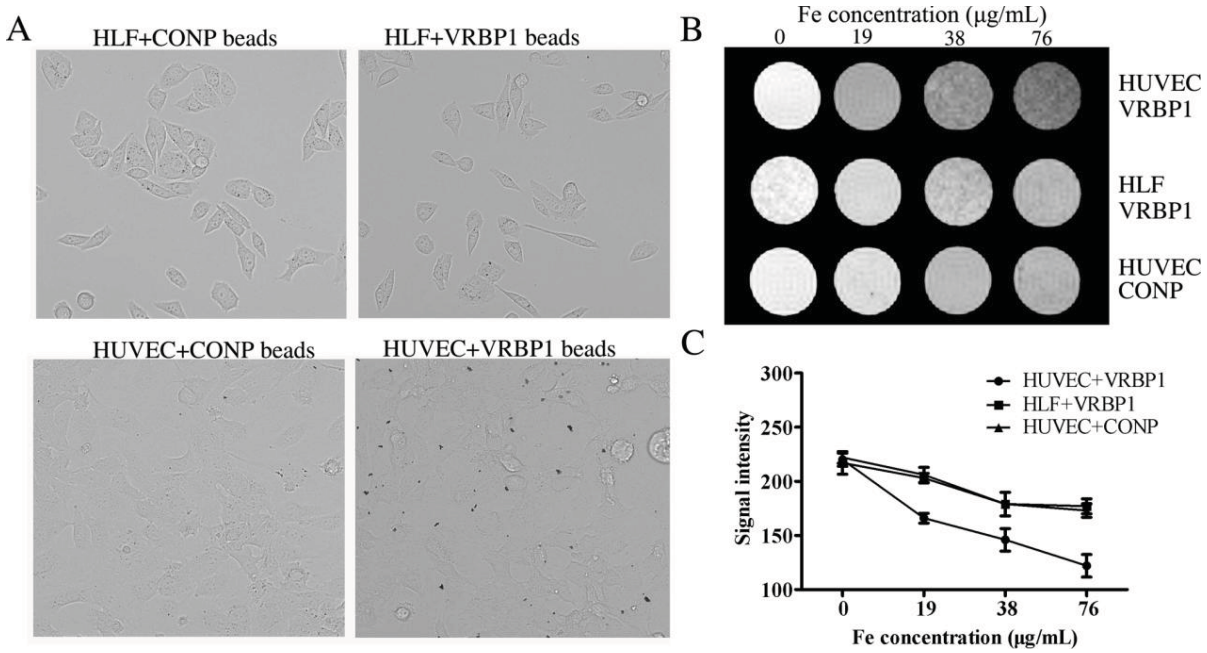

Fig. (4). Particles conjugated with VRBP1 could bind to HUVEC cells. (**A**) Carboxylic beads conjugated with VRBP1 accumulated on the surface of HUVEC cells. (**B**) T2-weighted imaging of HUVEC and HLF cells after incubated with SPIO-VRBP1 or SPIO-CONP at Fe concentration of 0, 19, 38, 76 μg/mL. (**C**) Quantification of MR signals intensity of HUVEC and HLF cells after incubated with SPIO-VRBP1 or SPIO-CONP.

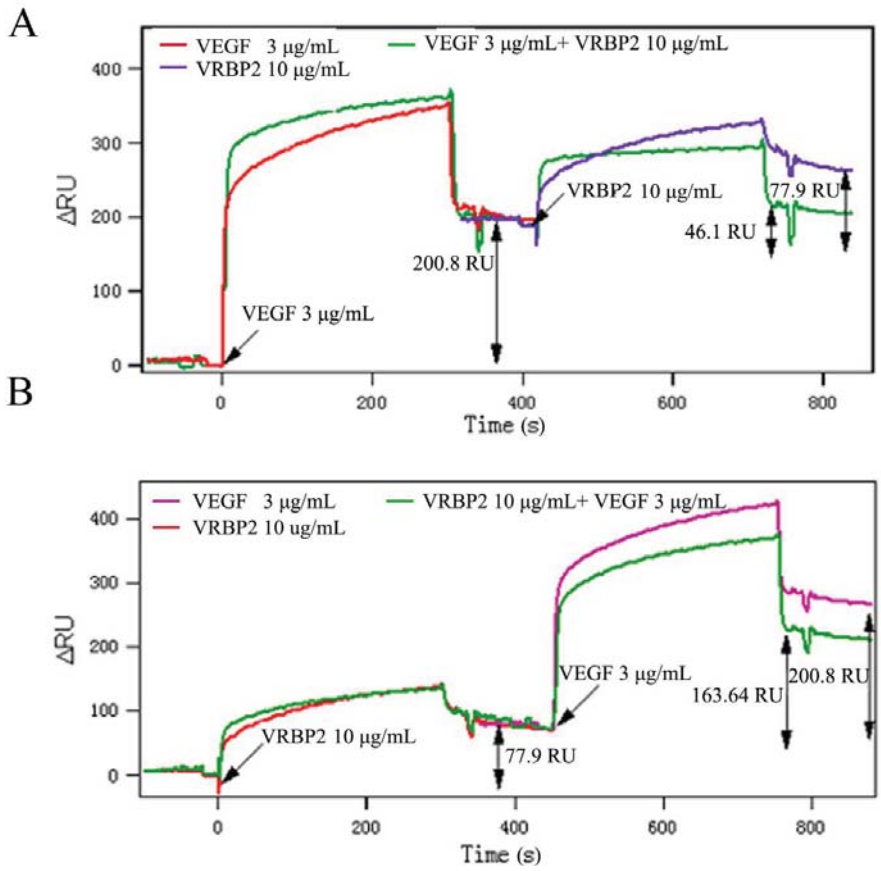

Fig. (5). VRBP1 blocked VEGF binding to its receptor VEGFR2 analyzed by SPR experiment. (A) VRBP1 at concentration of 10 μg/mL was introduced into the SPR reaction channel followed the binding of VEGF to VEGFR2. (B) VEGF at concentration of 3 μg/mL was introduced into the SPR reaction channel followedthe binding of VRBP1 to VEGFR2.

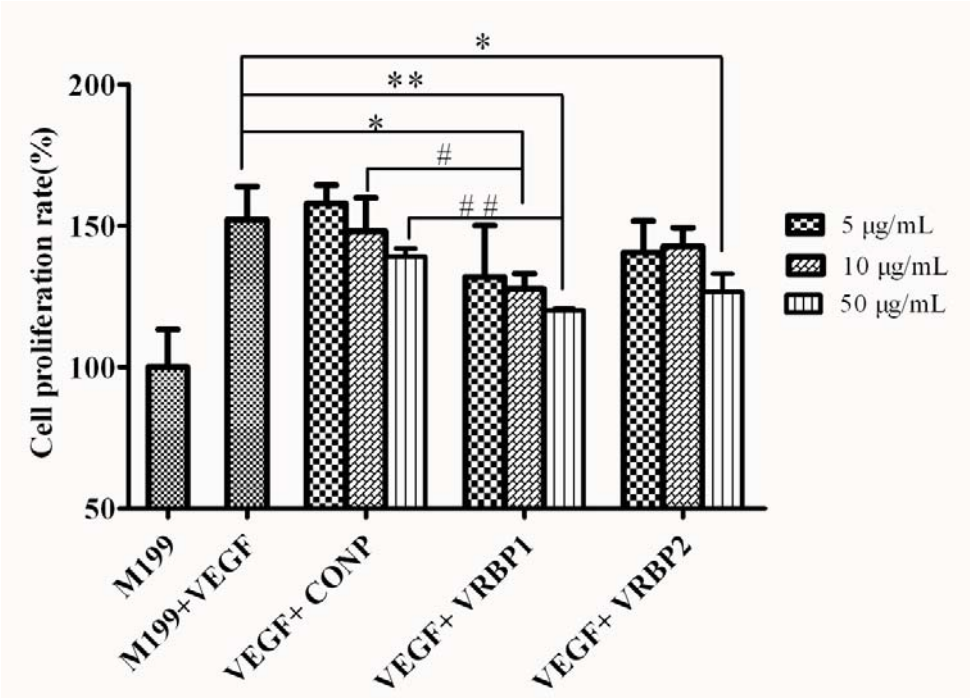

Fig. (6). VRBP1 could inhibit proliferation of HUVEC cells induced by VEGF at higher concentration. HUVEC cells treated with 30 ng/mL VEGF were separately co-incubated with CONP, VRBP1, and VRBP2 at various concentrations. Data were presented as mean ± S.D. of three independent experiments. Significance indicated by: *P<0.05 and **P<0.01 in comparison to VEGF treated HUVEC cells by Student's t-test; $^{\#}$P<0.05 and $^{\#\#}$P<0.01 in comparison to corresponding concentration of CONP co-incubated HUVEC cells by Student's t-test.

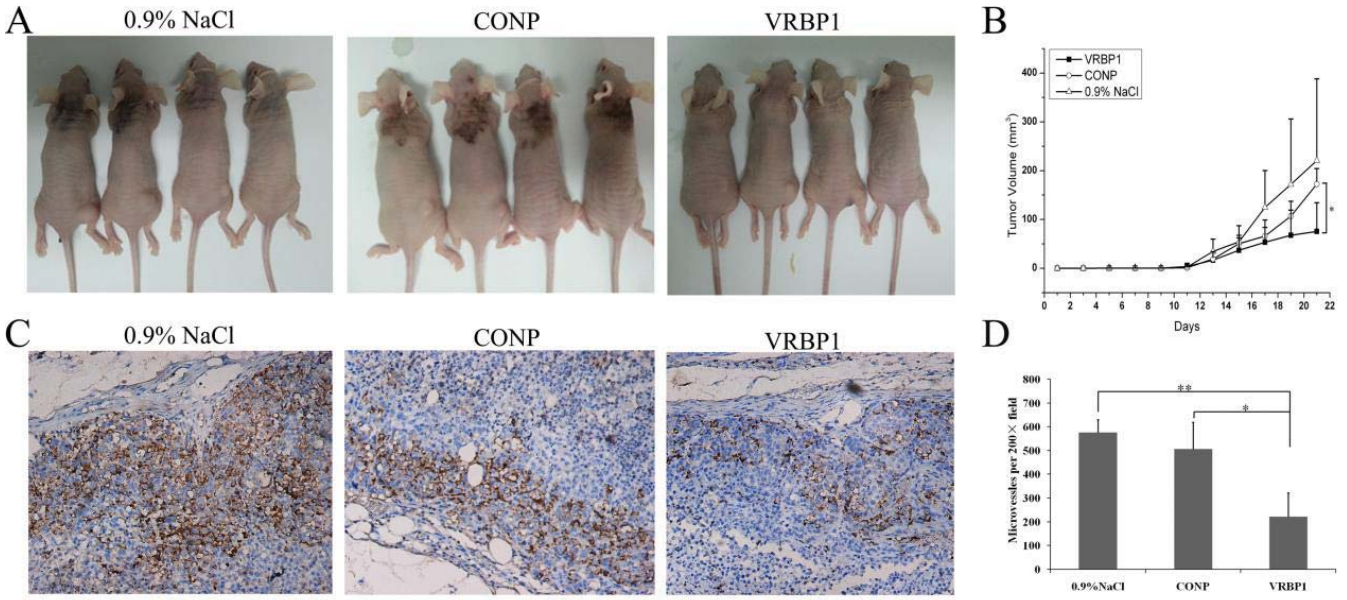

Fig. (7). VRBP1 suppressed tumor growth and angiogensis *in vivo*. (A) The images of mice loaded with tumors after treated with 100 μL 0.9% NaCl, CONP (400 μg/mL) and VRBP1 (400 μg/mL). (B) Tumor volumes of mice were recorded on the injection day. Data of tumor volumes were the mean value of four mice. *P<0.05 in comparison to CONP treated group by Student's t-test. (C) Images of CD31 immunostaining for tumor vasculature. (D) Quantification of the mean $CD31^+$ vessel number per 200× field [microvessel density (MVD)]. Data shown were the mean vessel counts of three paraffin sections. *P<0.05 in comparison to CONP treated group by Student's t-test; **P<0.01 in comparison to 0.9% NaCl treated group by Student's t-test.

and VRBP2 on the proliferation of HUVEC cells which over-expressed VEGFR2. As shown in Fig. **6**, VRBP1 significantly suppressed the mitogenic response of $rhVEGF_{165}$ to HUVEC cells at a concentration of 50 μg/mL. The less inhibitory effect on proliferation of HUVEC cells was observed by VRBP2 treatment. In order to verify the growth inhibition of VRBP1 that we observed in HUVEC cells, we performed similar experiments on HLF cells. The proliferation of HLF cells was not affected by VRBP1 (Fig. **S3**), indicating that the growth inhibitory effects of VRBP1 to HUVEC cells were not due to its potential cytotoxicity and the effect of peptides on HUVEC cells proliferation might be due to the blockade of the VEGF-VEGFR2 pathway by peptides.

VRBP1 Suppressed Tumor Growth and Angiogenesis *in vivo*

To examine the effect of VRBP1on tumor growth and angiogenesis *in vivo*, nu/nu mice with H460 tumor xenograft were used. One day after tumor xenograft was transplanted to mice, 100 μL VRBP1 (400 μg/mL) or CONP (400 μg/mL) or physiological saline was injected to tumor sites. The growth of tumors was assessed every other day. Our results (Fig. **7A**) indicated that VRBP1 could decrease the growth of tumor after 15 days compared with CONP and physiological saline group. The average tumor size in VRBP1 treated mice was around 75.47 mm^3, compared with 172.61 mm^3 in CONP group and 220.84 mm^3 in physiological saline group at 21 days post injection (Fig. **7B**), which indicated VRBP1 could decrease tumor size significantly compared to CONP. The effects of VRBP1 on angiogenesis were examined by immunohistochemical experiment. Serial sections from the solid tumors of nude mice with different treatments were incubated with CD31 antibody. The immunohistochemical results showed that there were more CD31 positive vessels presented in the physiological saline and CONP-treated tumor xenograft slides than those in the VRBP1 group (Fig. **7C**). Furthermore, sections from VRBP1 treated mice had a mean microvessel count of 221 per 200× field. For those sections from physiological saline and CONP treated mice, the corresponding value was 576 and 506 per 200× field (Fig. **7D**).

DISCUSSION

In our study, we successfully screened and selected the specific binding peptides for VEGFR2 with bacterial display method. Selected peptides in two different forms, peptides-bacteria and free peptides were characterized through examining their specificity and affinity to VEGFR2. VRBP1 obtained from focused library had higher affinity (K_D value was 228.3 nM) to VEGFR2 compared with the peptide (MAKGDFFERWGVKEM) (K_D value was 574.7 nM) from random library by the SPR assay (data not shown), which indicated that focused library with conserved sequences could promote to get better binding peptides for VEGFR2. Although the K_D value of peptide VRBP1 was not higher than that of antibodies, it was still in the acceptable range for the research and clinical usage. It could be understood since the molecular weight of peptides is smaller than that of antibodies, the force of hydrophobic between peptides and proteins may be weaker than that between antibodies and proteins [39]. Although the affinity between VRBP1 and VEGFR2 was less strong than that between VEGF and VEGFR2 [40], the competitive binding between VRBP1 and VEGF to VEGFR2 was observed from SPR assay and

confirmed by ELISA experiment. These results implied that VRBP1 might bind to VEGFR2 on the same or adjacent position as VEGF, which need to be verified in future. Through blocking the interaction between VEGF and VEGFR2, VRBP1 could defer the growth velocity of HUVEC cells, which meant that VRBP1 had the ability to block the function of VEGF on promoting the proliferation of HUVEC cells. Moreover, the tumor size and number of newly generated tumor vessels in the tumor xenograft models were reduced after the mice were injected with VRBP1. The results from these functional assays further proved that VRBP1 and VEGF competitively interacted with VEGFR2. Furthermore, we presented that VRBP1 could not only be used as therapeutic drugs for cancer patients potentially through inhibiting the growth of new vessels for cancers, but also for locale diagnosis of cancers after conjugating with SPIO.

Besides, peptides obtained from our study which could be used for cancer diagnosis and therapy, two robust tools were developed for the biotechnological research: 1. Affinity evaluation could be performed directly with the peptides on the surface of bacteria; 2. SPR method might substitute ELISA to examine the competitive relationship between various molecules.

Normally, isothermal titration calorimetry (ITC) [41], microscale thermophoresis (MST) [42, 43] and SPR [44] were often used to measure the K_D value of one molecule to the responding molecule. However, the successful measurement of these methods needs sophisticated machines and skillful technicians. In the preliminary section of the whole study, especially when the measurement objectives were very diverse, these methods were not suitable considering the cost and time. In our display system, peptides were displayed on the surface of bacteria, which could be considered as organism matrix. Provided that the expression level of any selected peptides on the bacteria surface was similar, when peptides-bacteria incubated with different concentrations of targeted fluorescent proteins, the fluorescent signals of bacteria had positive correlation with the binding rate between peptides and proteins. When we firstly designed this assay, the only thing expected was to get the relative comparative data about binding efficiency among different peptides with target proteins. Interestingly, from our data, the K_D values for selected peptides-bacteria were in the same mathematical level compared with those of same selected synthesized peptides from SPR measurement. It might prompt us that we could use this novel method to evaluate the K_D values of peptides to proteins.

As for the second useful tool developed from our study, we could use SPR method to substitute ELISA to examine the competitive relationship between different molecules to the same target. Antibodies and luminescent materials are the essential composites for ELISA experiments which implied that proteins/peptides need to be either labeled or used as luminescent antibodies in the system [45]. It is well known that SPR could be used to measure K_D values between two different molecules without any labels [46]. In theory, it could be used to examine the relationships between the two molecules when they could bind with the same target. However, there is no such report till now. In our study, we introduced the second molecule into the reaction channel when the first molecule finished interacting with the target protein without starting the washing procedure. The decreased reaction unit (SPR readout) presented between the second molecule and target proteins meant that these two molecules had competitive relationship binding to the target molecule. In our study, results from ELISA experiment and functional assays related to the peptides verified the validity of this method.

CONCLUSION

Taken together, in our study, peptides obtained from bacterial display methods could serve as powerful tools for both cancer diagnosis and therapy. Further verification of application for those peptides in clinic needs to be done in future. Besides that, two biotechnological tools developed would benefit the research in this area. We do hope that results from our study would have profound scientific and applicable value in both research and clinical fields.

SUPPLEMENTARY MATERIAL

Supplementary material is available on the publisher's web site along with the published article.

CONFLICT OF INTEREST

The authors confirm that this article content has no conflict of interest.

ACKNOWLEDGEMENTS

We thank Dr. Patrick S. Daugherty for providing bacterial display library. We are grateful to Dr. Biliang Zhang for providing cell lines. This work was funded by the National Natural Science Foundation of China (No. 81171451, 81372361 and 30870683).

LIST OF ABBREVIATIONS

BSA	=	bovine serum albumin
CM	=	chloramphenicol
DMEM/high	=	Dulbecco's modified Eagle's high glucose medium
DMSO	=	dimethyl sulfoxide
EDC	=	1-ethyl-3-(3-dimethylaminopropyl)-carbodiimide
ELISA	=	enzyme-linked immunosorbent assay
FACS	=	fluorescence-activated cell sorting
FBS	=	fetal bovine serum
FITC	=	fluorescein isothiocyanate
HLF	=	human lung fibroblast
HUVEC	=	human umbilical vein endothelial cells
ITC	=	isothermal titration calorimetry
K_D	=	dissociation constant
LB	=	lysogeny broth

MACS	=	magnetic-activated cell sorting
MES	=	2-(N-morpholino)-ethanesulfonic acid
MRI	=	magnetic resonance imaging
MSME	=	multi-slice multi-echo
MST	=	microscalethermophoresis
MTT	=	methyl thiazolyltetrazolium
MVD	=	microvessel density
M199	=	Medium 199
NHS	=	N-hydroxysuccinimide
OD	=	optical density
PBS	=	phosphate-buffered saline
$rhVEGF_{165}$	=	recombinant human $VEGF_{165}$
RU	=	response units
SAPE	=	streptavidin R-phycoerythrin
SOB	=	super optimal broth
SPIO	=	superparamagnetic iron oxide particle
SPR	=	surface plasmon resonance
STR	=	short tandem repeat
VEGF	=	vascular endothelial growth factor
VEGFR2	=	vascular endothelial growth factor receptor 2

REFERENCES

[1] Folkman, J. Angiogenesis in cancer, vascular, rheumatoid and other disease. *Nat. Med.,* **1995**, *1*(1), 27-31.

[2] Folkman, J. Seminars in medicine of the Beth Israel Hospital, Boston - Clinical applications of research on angiogenesis. *New Engl. J. Med.,* **1995**, *333*(26), 1757-1763.

[3] Papamichael, D. Prognostic role of angiogenesis in colorectal cancer. *Anticancer Res.,* **2000**, 21(6B), 4349-4353.

[4] Quesada, A.R.; Munoz-Chapuli, R.; Medina, M.A. Anti-angiogenic drugs: from bench to clinical trials. *Med. Res. Rev.,* **2006**, *26*(4), 483-530.

[5] Mittal, K.; Ebos, J.; Rini, B. Angiogenesis and the tumor microenvironment: vascular endothelial growth factor and beyond. *Semin. Oncol.,* **2014**, *41*(2), 235-251.

[6] Dimova, I.; Popivanov, G.; Djonov, V. Angiogenesis in cancer - general pathways and their therapeutic implications. *J. BUON,* **2014**, *19*(1), 15-21.

[7] Amini, A.; Masoumi Moghaddam, S.; Morris, D.L.; Pourgholami, M.H. The critical role of vascular endothelial growth factor in tumor angiogenesis. *Curr. Cancer Drug Targets,* **2012**, *12*(1), 23-43.

[8] Matthews, W.; Jordan, C.T.; Gavin, M.; Jenkins, N.A.; Copeland, N.G.; Lemischka, I.R. A receptor tyrosine kinase cDNA isolated from a population of enriched primitive hematopoietic cells and exhibiting close genetic linkage to c-kit. *Proc. Natl. Acad. Sci. U. S. A.,* **1991**, *88*(20), 9026-9030.

[9] Bry, M.; Kivela, R.; Leppanen, V.M.; Alitalo, K. Vascular Endothelial Growth Factor-B in Physiology and Disease. *Physiol. Rev.,* **2014**, *94*(3), 779-794.

[10] Shibuya, M. Vascular endothelial growth factor and its receptor system: physiological functions in angiogenesis and pathological roles in various diseases. *J. Biochem.,* **2013**, *153*(1), 13-19.

[11] Terman, B.I.; Dougher-Vermazen, M.; Carrion, M.E.; Dimitrov, D.; Armellino, D.C.; Gospodarowicz, D.; Bohlen, P. Identification of the KDR tyrosine kinase as a receptor for vascular endothelial cell growth factor. *Biochem. Biophys. Res. Commun.,* **1992**, *187*(3), 1579-1586.

[12] Su, J.L.; Chen, P.S.; Chien, M.H.; Chen, P.B.; Chen, Y.H.; Lai, C.C.; Hung, M.C.; Kuo, M.L. Further evidence for expression and function of the VEGF-C/VEGFR-3 axis in cancer cells. *Cancer Cell,* **2008**, *13*(6), 557-560.

[13] Mouawad, R.; Spano, J.P.; Comperat, E.; Capron, F.; Khayat, D. Tumoural expression and circulating level of VEGFR-3 (Flt-4) in metastatic melanoma patients: correlation with clinical parameters and outcome. *Eur. J. Cancer,* **2009**, *45*(8), 1407-1414.

[14] Carmeliet, P.; Jain, R.K. Molecular mechanisms and clinical applications of angiogenesis. *Nature,* **2011**, *473*(7347), 298-307.

[15] Simons, M. An inside view: VEGF receptor trafficking and signaling. *Physiology,* **2012**, *27*(4), 213-222.

[16] Spannuth, W.A.; Nick, A.M.; Jennings, N.B.; Armaiz-Pena, G.N.; Mangala, L.S.; Danes, C.G.; Lin, Y.G.; Merritt, W.M.; Thaker, P.H.; Kamat, A.A.; Han, L.Y.; Tonra, J.R.; Coleman, R.L.; Ellis, L.M.; Sood, A.K. Functional significance of VEGFR-2 on ovarian cancer cells. *Int. J. Cancer,* **2009**, *124*(5), 1045-1053.

[17] Mao, W.F.; Shao, M.H.; Gao, P.T.; Ma, J.; Li, H.J.; Li, G.L.; Han, B.H.; Yuan, C.G. The important roles of RET, VEGFR2 and the RAF/MEK/ERK pathway in cancer treatment with sorafenib. *Acta Pharmacol. Sin.,* **2012**, *33*(10), 1311-1318.

[18] Sharma, P.S.; Sharma, R.; Tyagi, T. VEGF/VEGFR pathway inhibitors as anti-angiogenic agents: present and future. *Curr. Cancer Drug Targets,* **2011**, *11*(5), 624-653.

[19] Wilhelm, S.M.; Carter, C.; Tang, L.; Wilkie, D.; McNabola, A.; Rong, H.; Chen, C.; Zhang, X.; Vincent, P.; McHugh, M.; Cao, Y.; Shujath, J.; Gawlak, S.; Eveleigh, D.; Rowley, B.; Liu, L.; Adnane, L.; Lynch, M.; Auclair, D.; Taylor, I.; Gedrich, R.; Voznesensky, A.; Riedl, B.; Post, L.E.; Bollag, G.; Trail, P.A. BAY 43-9006 exhibits broad spectrum oral antitumor activity and targets the RAF/MEK/ERK pathway and receptor tyrosine kinases involved in tumor progression and angiogenesis. *Cancer Res.,* **2004**, *64*(19), 7099-7109.

[20] Adams, G.P.; Weiner, L.M. Monoclonal antibody therapy of cancer. *Nat. Biotechnol.,* **2005**, *23*(9), 1147-1157.

[21] Vlieghe, P.; Lisowski, V.; Martinez, J.; Khrestchatisky, M. Synthetic therapeutic peptides: science and market. *Drug Discov. Today,* **2010**, *15*(1-2), 40-56.

[22] Falciani, C.; Lelli, B.; Brunetti, J.; Pileri, S.; Cappelli, A.; Pini, A.; Pagliuca, C.; Ravenni, N.; Bencini, L.; Menichetti, S.; Moretti, R.; De Prizio, M.; Scatizzi, M.; Bracci, L. Modular branched neurotensin peptides for tumor target tracing and receptor-mediated therapy: A Proof-of-concept. *Curr. Cancer Drug Targets,* **2010**, *10*(7), 695-704.

[23] Kaspar, A.A.; Reichert, J.M. Future directions for peptide therapeutics development. *Drug Discov. Today,* **2013**, *18*(17-18), 807-817.

[24] Molek, P.; Strukelj, B.; Bratkovic, T. Peptide phage display as a tool for drug discovery: targeting membrane receptors. *Molecules,* **2011**, *16*(1), 857-887.

[25] Hamzeh-Mivehroud, M.; Alizadeh, A.A.; Morris, M.B.; Bret Church, W.; Dastmalchi, S. Phage display as a technology delivering on the promise of peptide drug discovery. *Drug Discov. Today,* **2013**, *18*(23–24), 1144-1157.

[26] Gordon, E.M.; Barrett, R.W.; Dower, W.J.; Fodor, S.P.; Gallop, M.A. Applications of combinatorial technologies to drug discovery. 2. Combinatorial organic synthesis, library screening strategies, and future directions. *J. Med. Chem.,* **1994**, *37*(10), 1385-1401.

[27] Lei, H.; An, P.; Song, S.; Liu, X.; He, L.; Wu, J.; Meng, L.; Liu, M.; Yang, J.; Shou, C. A novel peptide isolated from a phage display library inhibits tumor growth and metastasis by blocking the binding of vascular endothelial growth factor to its receptor KDR. *J. Biol. Chem.,* **2002**, *277*(45), 43137-43142.

[28] Binetruy-Tournaire, R.; Demangel, C.; Malavaud, B.; Vassy, R.; Rouyre, S.; Kraemer, M.; Plouet, J.; Derbin, C.; Perret, G.; Mazie, J.C. Identification of a peptide blocking vascular endothelial growth factor (VEGF)-mediated angiogenesis. *EMBO J.* **2000**, *19*(7), 1525-1533.

[29] Bessette, P.H.; Rice, J.J.; Daugherty, P.S. Rapid isolation of high-affinity protein binding peptides using bacterial display. *Protein Eng. Des. Sel.,* **2004**, *17*(10), 731-739.

[30] Becker, S.; Schmoldt, H.U.; Adams, T.M.; Wilhelm, S.; Kolmar, H. Ultra-high-throughput screening based on cell-surface display and fluorescence-activated cell sorting for the identification of novel biocatalysts. *Curr. Opin. Biotechnol.,* **2004**, *15*(4), 323-329.

[31] Dong, B.; Wang, A.; Yuan, L.; Chen, L.; Pu, K.; Duan, W.; Yan, X.; Zhu, Y. Peptide-fluorescent bacteria complex as luminescent reagents for cancer diagnosis. *PLoS One,* **2013**, *8*(1), e54467.

[32] Erdag, B.; Balcioglu, K.B.; Kumbasar, A.; Celikbicak, O.; Zeder-Lutz, G.; Altschuh, D.; Salih, B.; Baysal, K. Novel short peptides isolated from phage display library inhibit vascular endothelial growth factor activity. *Mol. Biotechnol.,* **2007**, *35*(1), 51-63.

[33] Rice, J.J.; Daugherty, P.S. Directed evolution of a biterminal bacterial display scaffold enhances the display of diverse peptides. *Protein Eng. Des. Sel.,* **2008**, *21*(7), 435-442.

[34] Yang, T.; Wu, Y.; Zhang, X.; Zhang, Y.; Gu, N. Effect of surface modifications on the peroxidase-like activity of iron oxide nanoparticles. *J. Southeast Univ. (Med. Sci. Edi.),* **2009**, 29, 242-247.

[35] Maruyama, Y. The human endothelial cell in tissue culture. *Z. Zellforsch. Mikrosk. Anat.,* **1963**, *60*(1), 69-79.

[36] Jiménez, N.; Krouwer, V.J.; Post, J.A. A new, rapid and reproducible method to obtain high quality endothelium *in vitro*. *Cytotechnology,* **2013**, *65*(1), 1-14.

[37] Kenrick, S.A.; Daugherty, P.S. Bacterial display enables efficient and quantitative peptide affinity maturation. *Protein Eng. Des. Sel.,* **2010**, *23*(1), 9-17.

[38] Nguyen, A.W.; Daugherty, P.S. Evolutionary optimization of fluorescent proteins for intracellular FRET. *Nat. Biotechnol.,* **2005**, *23*(3), 355-360.

[39] Cserháti, T.; Szögyi, M. Role of hydrophobic and hydrophilic forces in peptide-protein interaction: new advances. *Peptides,* **1995**, *16*(1), 165-173.

[40] Udugamasooriya, D.G.; Dineen, S.P.; Brekken, R.A.; Kodadek, T. A peptoid "antibody surrogate" that antagonizes VEGF receptor 2 activity. *J. Am. Chem. Soc.,* **2008**, *130*(17), 5744-5752.

[41] Burnouf, D.; Ennifar, E.; Guedich, S.; Puffer, B.; Hoffmann, G.; Bec, G.; Disdier, F.; Baltzinger, M.; Dumas, P. kinITC: A new method for obtaining joint thermodynamic and kinetic data by isothermal titration calorimetry. *J. Am. Chem. Soc.,* **2011**, *134*(1), 559-565.

[42] Seidel, S.A.; Wienken, C.J.; Geissler, S.; Jerabek-Willemsen, M.; Duhr, S.; Reiter, A.; Trauner, D.; Braun, D.; Baaske, P. Label-Free Microscale Thermophoresis Discriminates Sites and Affinity of Protein–Ligand Binding. *Angew. Chem. Int. Ed.,* **2012**, *51*(42), 10656-10659.

[43] Wienken, C.J.; Baaske, P.; Rothbauer, U.; Braun, D.; Duhr, S. Protein-binding assays in biological liquids using microscale thermophoresis. *Nat. Commun.,* **2010**, *1*, 100.

[44] Lynch, H.E.; Stewart, S.M.; Kepler, T.B.; Sempowski, G.D.; Alam, S.M. Surface plasmon resonance measurements of plasma antibody avidity during primary and secondary responses to anthrax protective antigen. *J. Immunol. Methods,* **2014**, *404*, 1-12.

[45] Gan, S.D.; Patel, K.R. Enzyme immunoassay and enzyme-linked immunosorbent assay. *J. Invest. Dermatol.,* **2013**, *133*(9), e12.

[46] Gunzburg, M.J.; Ambaye, N.D.; Hertzog, J.T.; Del Borgo, M.P.; Pero, S.C.; Krag, D.N.; Wilce, M.C.; Aguilar, M.; Perlmutter, P., Wilce, J.A. Use of SPR to Study the Interaction of G7-18NATE Peptide with the Grb7-SH2 Domain. *Int. J. Pept. Res. Ther.,* **2010**, *16*(3), 177-184.

Received: July 22, 2014 Revised: January 06, 2015 Accepted: January 19, 2015